Specific deletion of focal adhesion kinase suppresses tumor formation and blocks malignant progression

Specific deletion of focal adhesion kinase suppresses tumor formation and blocks malignant progression

Gordon W. McLean,[1,8] Noboru H. Komiyama,[3,4] Bryan Serrels,[1] Hidefumi Asano,[4,7] Louise Reynolds,[5] Francesco Conti,[5] Kairbaan Hodivala-Dilke,[5] Daniel Metzger,[6] Pierre Chambon,[6] Seth G.N. Grant,[3,4] and Margaret C. Frame[1,2]

[1]The Beatson Institute for Cancer Research, Garscube Estate, Bearsden, Glasgow, G61 1BD, United Kingdom; [2]Institute of Biological and Life Sciences, University of Glasgow, Glasgow G12 8QQ, United Kingdom; [3]Wellcome Trust Sanger Institute, Cambridgeshire, CB10 1XA, United Kingdom; [4]Division of Neuroscience, University of Edinburgh, Edinburgh, EH8 9JZ, United Kingdom; [5]The London Queen Mary's School of Medicine and Dentistry, John Vane Science Centre, London, EC1M 6BQ, United Kingdom; [6]Institut de Génétique et de Biologie Moléculaire et Cellulaire, CNRS/INSERM/ULP, Collège de France, 67404 Illkirch Cedex, Strasbourg, France

We have generated mice with a floxed *fak* allele under the control of keratin-14-driven *Cre* fused to a modified estrogen receptor (*Cre*ER^{T2}). 4-Hydroxy-tamoxifen treatment induced *fak* deletion in the epidermis, and suppressed chemically induced skin tumor formation. Loss of *fak* induced once benign tumors had formed inhibited malignant progression. Although *fak* deletion was associated with reduced migration of keratinocytes in vitro, we found no effect on wound re-epithelialization in vivo. However, increased keratinocyte cell death was observed after *fak* deletion in vitro and in vivo. Our work provides the first experimental proof implicating FAK in tumorigenesis, and this is associated with enhanced apoptosis.

Supplemental material is available at http://www.genesdev.org.

Received July 1, 2004; revised version accepted October 14, 2004.

Cellular focal adhesions are complex structures consisting of many interacting proteins that provide both physical adhesion to extracellular matrix, usually via transmembrane integrin receptors, and that also transmit survival and/or growth signals into the cell interior. Deregulation of these adhesions may permit cancer cells to migrate and invade into surrounding tissue during the development of malignant disease, or to survive and grow under normally inappropriate conditions. One major component of integrin adhesions is focal adhesion kinase (FAK), a nonreceptor tyrosine kinase that is pivotal in many signaling pathways (Ilic et al. 1997). FAK regulates integrin-mediated adhesion and cell migration, and contributes to proliferation and cell survival (Schaller 2001; Hauck et al. 2002). Despite numerous reports that FAK expression correlates with the development of cancer (Owens et al. 1995, 1996; Agochiya et al. 1999; Jones et al. 2000; McLean et al. 2003), there is no direct evidence whether, and if so how, FAK contributes to cancer development.

Using *fak* heterozygous (+/–) mice, we previously demonstrated that reduced FAK expression had a negative impact on chemically induced papilloma formation (McLean et al. 2001). However, these benign tumors from $fak^{+/-}$ mice elevated expression of FAK to a level that was indistinguishable from papillomas from wild-type $fak^{+/+}$ mice, preventing us from addressing the key question of whether FAK expression is causally involved in malignant progression. Here, we address whether FAK plays a causal role in development of the malignant phenotype in vivo, by generating mice in which we had both spatial and temporal control over *fak* deletion. Specifically, we used gene targeting in embryonic stem (ES) cells to generate mice that are homozygous for a floxed *fak* allele, and that also express a 4-hydroxy-tamoxifen (4-OHT)-regulated *Cre* recombinase (*Cre*-ER^{T2}) expressed under control of the keratin-14 promoter (K14*Cre*ER^{T2}/FAK$^{flox/flox}$). We could delete *fak* from the epidermis of these mice upon addition of 4-OHT, but more importantly from benign papilloma tumors once these had developed. Our results provide the first evidence that FAK modulates the efficiency of benign tumor formation and plays a crucial role in malignant conversion.

Results and Discussion

To investigate the role of FAK during the formation and development of skin tumors, we used *Cre/lox*P technology to target the introduction of conditional mutations into the *fak* gene in mice. As the *fak* coding exons are spread over >225 kb, it was not practical to *flox* the entire *fak* gene; instead, *lox*P sites were introduced into the *fak* gene at positions flanking the exon encoding part of the kinase domain, that is, FAK amino acids 413–444. (The gene-targeting strategy and generation of FAK floxed mice are described in detail in the Supplemental Material.) The targeting vector was designed so that *Cre*-mediated recombination also introduced a frameshift mutation in the adjacent exon, precluding production of a functional FAK protein. Screening of *Cre*-expressing ES cells by immunoblotting confirmed that no FAK protein was detectable (Fig. 1A). Using N-terminal antibodies to FAK, no truncated products were visualized (data not shown). To obtain epidermal-specific *fak* excision, we crossed homozygous FAK$^{flox/flox}$ mice with mice expressing a modified estrogen receptor–*Cre* fusion protein (*Cre*ER^{T2}) (Indra et al. 1999), under the control of the keratin-14 (K14) promoter. This directs 4-OHT-induced excision of floxed *fak* to epidermal keratinocytes of mouse skin (Indra et al. 1999; Li et al. 2000). The resulting K14*Cre*ER^{T2}/FAK$^{flox/flox}$ mice were viable and dis-

[*Keywords*: Focal adhesion kinase; conditional; cancer; keratinocyte; apoptosis]
[7]**Present address: Chiba-City Kaihin Hospital, 3-31-1 Isobe, Mihama-Ku, Chiba City, Japan.**
[8]**Corresponding author.**
E-MAIL g.mclean@beatson.gla.ac.uk; FAX 44-141-942-6521.
Article and publication are at http://www.genesdev.org/cgi/doi/10.1101/gad.316304.

played skin-specific suppression of FAK expression following administration of 4-OHT, while other tissues, such as kidney and spleen, remained unaffected (Fig. 1B). Although some FAK was also detected in immunoblots of epidermal extracts from 4-OHT-treated animals (Fig. 1B, lane 6), this is most likely due to FAK expression in the underlying dermis that contaminates the epidermal preparations, or to the presence of a small number of keratinocytes that had not undergone FAK deletion due to loss of K14 expression through differentiation (Stoler et al. 1988). Immunohistochemistry revealed reduced FAK expression in both the epidermis and hair follicles of K14*Cre*ER^{T2}/FAK$^{flox/flox}$ mice, when compared with underlying dermis (Fig. 1C). This temporally controlled deletion of *fak* allowed separation of effects on benign tumor formation from those on malignant conversion.

Skin tumors were induced in 4-OHT-treated and untreated K14*Cre*ER^{T2}/FAK$^{flox/flox}$ mice by a two-stage chemical carcinogenesis protocol (Quintanilla et al. 1986; Kemp et al. 1993; Yuspa et al. 1995), as well as in K14*Cre*ER^{T2} and 4-OHT-treated FAK$^{flox/flox}$ mice to rule out possible effects of *Cre* expression or 4-OHT treatment, respectively. Treatment with the carcinogen 7,12-dimethylbenzanthracene (DMBA) gives rise to activating mutation of the c-Ha-Ras gene (Quintanilla et al. 1986; Pelling et al. 1987), and subsequent treatment for 20 wk with the tumor promoter 12-O-tetradecanoylphorbol-13-acetate (TPA) leads to formation of benign papillomas, a proportion of which progress to form invasive squamous cell carcinomas (SCC) (Burns et al. 1978). We observed a marked difference in papilloma formation between 4-OHT-treated and untreated K14*Cre*ER^{T2}/FAK$^{flox/flox}$ mice. Only 50% of 4-OHT-treated mice formed papillomas after 12 wk, as compared to 100% of untreated mice (Fig. 1D). More significantly, there was also a substantial reduction in the average number of papillomas formed per 4-OHT-treated K14*Cre*ER^{T2}/FAK$^{flox/flox}$ mouse at 22 wk when compared to the untreated control group (Fig. 1E). Additionally, no difference in benign tumor acquisition was observed in either the K14*Cre*ER^{T2} or the 4-OHT-treated FAK$^{flox/flox}$ mice ruling out any possible effects of *Cre* expression or 4-OHT treatment, respectively (data not shown). This indicates that FAK plays a modulatory role in chemically induced, Ras-dependent papilloma formation, with half of the 4-OHT-treated K14*Cre*ER^{T2}/FAK$^{flox/flox}$ mice being resistant to DMBA/TPA-induced benign tumor formation. We have reported previously that keratinocytes derived from *fak*$^{+/-}$ heterozygous mice display impaired signaling to Ras effector pathways (McLean et al. 2001), such as ERK/MAP kinase. Taken with our current findings, the data indicate that FAK is necessary not only for the biochemical effects of Ras in cells in culture, but also for optimal tumor initiating/promoting biological effects of oncogenic Ras in vivo.

Experiments using immortalized *fak*$^{-/-}$ mouse embryo fibroblasts have implicated FAK in migration and invasion (Ilic et al. 1995), while FAK expression in tumors correlates with invasive potential (Owens et al. 1995). However, owing to the embryonic lethality of constitutive *fak* deletion (Ilic et al. 1995), no experiments have been done to test whether FAK has a causal role in the development of malignancy per se. We therefore deleted *fak* directly from preformed benign papillomas and examined subsequent progression to invasive SCC tumors. K14*Cre*ER^{T2}/FAK$^{flox/flox}$ mice were subjected to DMBA and TPA, and subsequently treated with 4-OHT after the majority of papillomas had formed (at 15 wk as indicated in Fig. 2A). Immunohistochemistry confirmed *fak* gene excision after 4-OHT treatment, as judged by loss of specific FAK staining in hyperproliferative epidermal regions of papilloma sections (Fig. 2B, right panel). As judged by visual identification and subsequent histological confirmation of SCC, 4.1% of papillomas

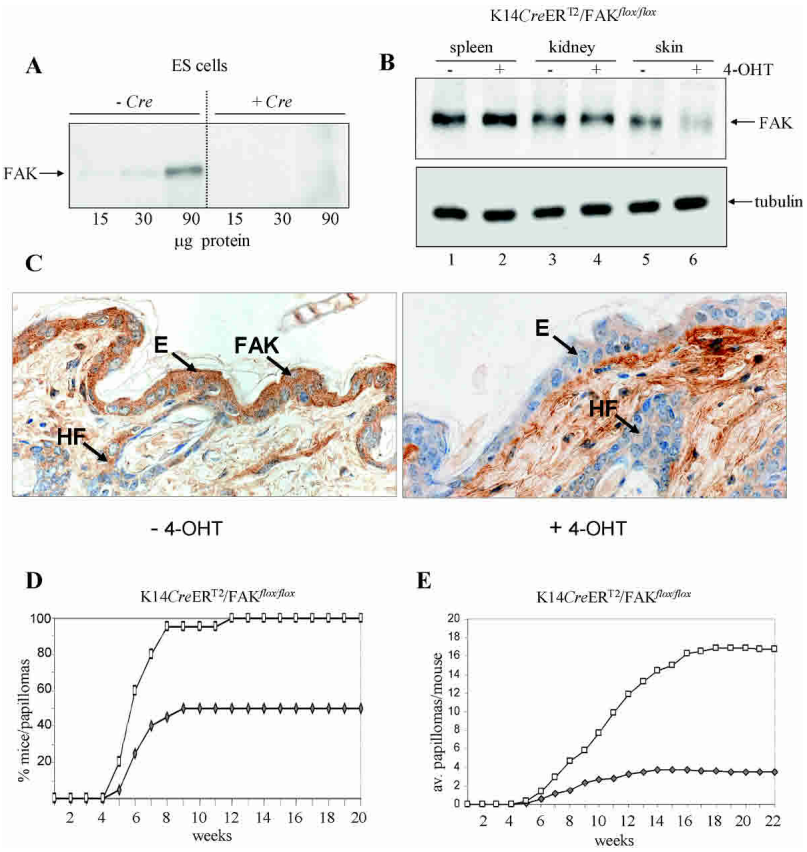

Figure 1. Deletion of FAK from mouse skin blocks papilloma formation. (*A*) *fak* excision in ES cells following introduction of *Cre* recombinase. *Cre* was introduced by electroporation of a pMC1-*Cre* plasmid, and protein extracts were harvested and subjected to Western blotting with an FAK mAb. (Lanes *1–3*) No *Cre* recombinase. (Lanes *4–6*) *Cre* recombinase. (*B*) Proteins were harvested from spleen, kidney, and skin of K14*Cre*ER^{T2}/FAK$^{flox/flox}$ mice either treated with 4-OHT or with vehicle alone. Extracts were blotted onto nitrocellulose and probed with an anti-FAK mAB (*top* panel) or an anti-tubulin mAB (*lower* panel). (*C*) Immunohistochemical staining of paraffin-embedded skin sections from K14*Cre*ER^{T2}/FAK$^{flox/flox}$ mice treated with either 4-OHT (*right* panel) or vehicle alone (*left* panel). (E) Epidermis; (HF) hair follicles. Deletion of *fak* in epidermal keratinocytes in vivo inhibits papilloma formation during chemical carcinogenesis. Mice were either treated with 4-OHT (♦) or vehicle alone (□) and subjected to DMBA and TPA treatment as described. Graphs indicate percent of mice acquiring papillomas over time (*D*) and average numbers of papillomas recorded per mouse over treatment time (*E*). Graphs represent K14*Cre*ER^{T2}/FAK$^{flox/flox}$ mice.

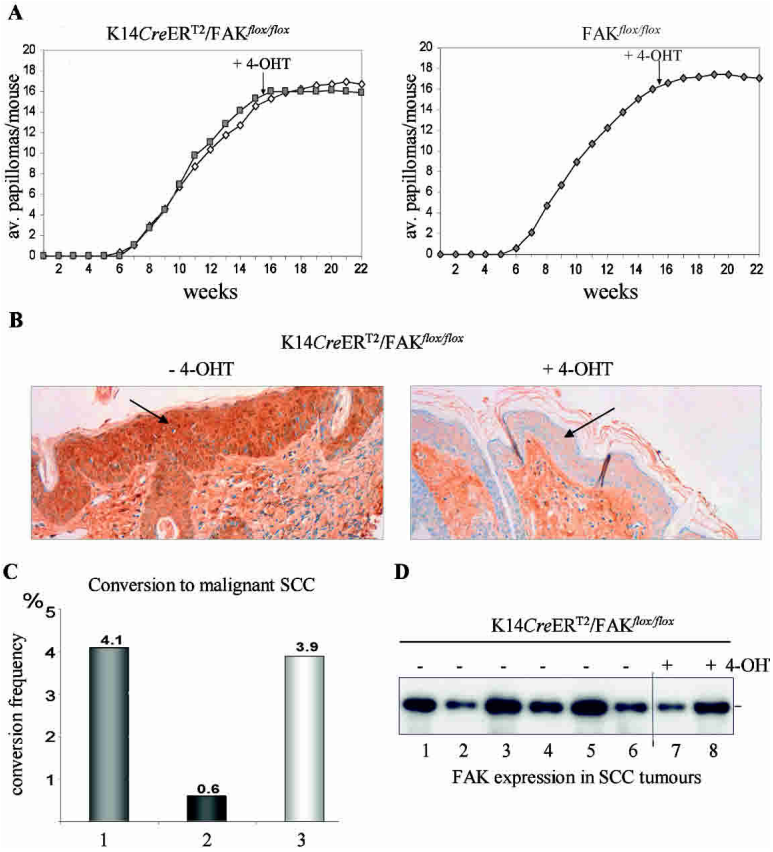

Figure 2. Deletion of *fak* from papillomas blocks malignant progression to SCC. (*A*) Mice either K14*Cre*ER^{T2}/FAK$^{flox/flox}$ (*left* panel) or FAK$^{flox/flox}$ (*right* panel) were treated with vehicle alone or with 4-OHT (+4-OHT) at 15 wk after the majority of papillomas had formed. (*B*) Immunohistochemical anti-FAK staining of paraffin-embedded sections of papillomas from K14*Cre*ER^{T2}/FAK$^{flox/flox}$ mice treated with vehicle alone (*left* panel) and with 4-OHT (*right* panel). (*C*) Papilloma to carcinoma conversion frequency of 4-OHT-treated and untreated K14*Cre*ER^{T2}/FAK$^{flox/flox}$ mice (1 and 2) and 4-OHT-treated FAK$^{flox/flox}$ mice (3). Conversion frequency is determined by calculating the number of carcinomas recorded per total number of papillomas for each study group. (*D*) Anti-FAK immunoblot of proteins extracted from SCCs derived from untreated (lanes *1–6*) or 4-OHT-treated (lanes *7,8*) K14*Cre*ER^{T2}/FAK$^{flox/flox}$ mice.

underwent conversion to carcinoma in untreated mice, whereas malignant conversion of papillomas in 4-OHT-treated K14*Cre*ER^{T2}/FAK$^{flox/flox}$ mice was reduced to 0.6% (Fig. 2C). An observed conversion frequency of 3.9% in 4-OHT-treated FAK$^{flox/flox}$ mice excluded the possibility of this observation being linked to administration of 4-OHT (Fig. 2C). The 0.6% conversion frequency represented two SCCs that developed in 4-OHT-treated K14*Cre*ER^{T2}/FAK$^{flox/flox}$ mice, and subsequent immunoblotting of lysates prepared from these tumors demonstrated retention of FAK expression at levels in the same range as SCCs developed from untreated K14*Cre*ER^{T2}/FAK$^{flox/flox}$ mice (Fig. 2D, lanes 7,8). Therefore, these two SCCs had arisen from papillomas in which the *fak* gene had not been excised by 4-OHT treatment. Crucially, FAK-deficient SCCs never arose during our experiments, implying that loss of FAK expression from the hyperproliferative epidermal region of papillomas is incompatible with malignant progression.

Deriving keratinocytes from K14*Cre*ER^{T2}/FAK$^{flox/flox}$ mice allowed us to examine the effects of *fak* deletion in the normal epithelial cells that are the targets for tumorigenesis in the DMBA/TPA skin carcinogenesis model. This provides important advantages over the commonly used *fak*$^{-/-}$ cells (Ilic et al. 1995), not only because the latter are mesenchymal but also because they are deficient in p53 that might influence their behavior (Ilic et al. 1995). Peripheral FAK staining was visible in untreated keratinocytes, presumably at integrin adhesion sites that represent keratinocyte focal adhesions, whereas 4-OHT treatment caused loss of peripheral FAK staining in the majority of cells (Fig. 3A). The small number of cells that continue to express FAK may be due to suppression of K14 expression that may occur as keratinocytes differentiate (Fig. 3A, right panel, arrow; Stoler et al. 1988). We first carried out wound repair migration assays, and found that 4-OHT-treated K14*Cre*ER^{T2}/FAK$^{flox/flox}$ keratinocytes were unable to repopulate the denuded areas of wounded monolayers when compared to control cultures (Fig. 3B). To address whether this could be explained by defective cell migration, we tracked individual cells using time-lapse microscopy and found that *fak*$^{-/-}$ keratinocytes displayed reduced migration rates (by ~50%), but they were still visibly motile (Fig. 3C). However, we noticed that there were fewer cells present even in the confluent regions at the wound edges after 48 h (Fig. 3B, arrows), suggesting that failure to repair the wound in vitro may be associated with detachment and/or cell death. We collected adherent and detached cells following treatment with 4-OHT and determined the proportion of cells with sub-2n DNA content by FACS analysis. We found that loss of FAK was associated with loss of normal cell cycle profiles and a substantial amount of cell death when compared with untreated primary keratinocytes (Fig. 3D,E).

Our data thus provide the first direct experimental evidence that FAK causally contributes to the development of malignancy in vivo, specifically during the benign papilloma to SCC transition. Furthermore, this is associated with a requirement for FAK to maintain a normal rate of cell migration, and survival signaling in keratinocytes in vitro. To determine which, if either, of these effects is likely to be responsible for the observed suppression of tumorigenesis upon FAK deletion, we carried out punch biopsy wound repair assays and analyzed caspase-3 activation in 4-OHT-treated K14*Cre*ER^{T2}/FAK$^{flox/flox}$ skin to monitor in vivo migration and apoptosis, respectively. K14*Cre*ER^{T2}/FAK$^{flox/flox}$ mice (either treated or untreated with 4-OHT) were wounded with 3-mm punch biopsies (Fig. 4A, day 0, upper panels), and subsequent wound closure was monitored. No visible difference in in vivo wound repair was observed—as judged at 7 d after wounding—when re-epithelialization was essentially complete in both cases (Fig. 4A, day 7, lower panels). Earlier time points at days 1 and 3 did not indicate any lag in re-epithelialization of the wounded skin (data not shown). In contrast, we observed a difference in staining of activated caspase-3 both in the skin and in papillomas

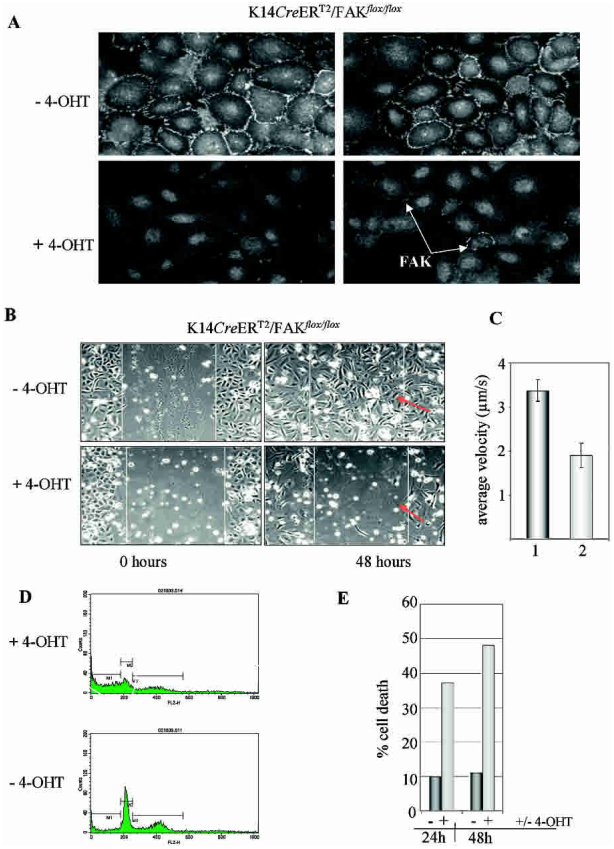

Figure 3. Deletion of FAK from keratinocytes causes reduced migration and increased cell death. (*A*) Confocal images show anti-FAK staining of peripheral structures in untreated (–4-OHT) or treated (+4-OHT) keratinocytes derived from K14*Cre*ER^{T2}/FAK$^{flox/flox}$ mice. Arrows indicate FAK staining in a minority of treated keratinocytes. Images were taken following 48 h of 4-OHT treatment. (*B*) Phase-contrast images show in vitro wound-repair assays of untreated (–4-OHT) or treated (+4-OHT) keratinocytes derived from K14*Cre*ER^{T2}/FAK$^{flox/flox}$ mice at 0 h and 48 h after the wound was made in the monolayer. Arrows indicate areas of the monolayer at the edges of the wound after 48 h. (*C*) Migration rates of keratinocytes derived from FAK$^{flox/flox}$ mice (1) and K14*Cre*ER^{T2}/FAK$^{flox/flox}$ mice (2), treated with 4-OHT for 48 h, were determined by time-lapse cell tracking and migration rate software analysis expressed as average speed in microns per second. (*D*,*E*) Cell death of untreated (–4-OHT) or treated (+4-OHT) keratinocytes derived from K14*Cre*ER^{T2}/FAK$^{flox/flox}$ mice was judged by the percentage of cells with sub-2n DNA content by FACS analysis; 24 h and 48 h refers to the time of sample collection after wounding.

from treated, but not untreated, mice (Fig. 4B). Activated caspase-3 is accepted as a key marker of apoptotic cells and is now widely considered to be a more reliable indicator of apoptosis in tissue sections than TUNEL staining (Marshman et al. 2001; Duan et al. 2003). In particular, we observed the strongest staining in cells of the hair follicles of 4-OHT-treated mice, where the majority of target cells for DMBA-induced tumorigenesis are thought to reside (Fig. 4B, middle panels; Argyris 1980). Moreover, FAK deletion from preformed benign papillomas caused stronger staining of active caspase-3 (Fig. 4B, lower panels). Thus, it is FAK's role in promoting cell survival that is tightly linked to tumor formation and progression in this mouse.

This, together with the increased expression of FAK during acquisition of malignancy (Owens et al. 1995; McLean et al. 2003), is in keeping with recent observations that FAK can promote invasion in vitro by regulating production of matrix metalloproteinases (Shibata et al. 1998; Hauck et al. 2002). We have now causally implicated FAK as a determinant of malignant behavior in vivo, identifying FAK as an excellent candidate for further study as a potential target to suppress spread of the disease.

Materials and methods

Animals and gene targeting

Design, construction, and generation of mice containing targeted *lox*P sites in the FAK gene are described in detail in the Supplemental Material. Transgenic mice expressing the modified *Cre* recombinase–estrogen receptor fusion under control of the keratin-14 promoter (K14*Cre*ER^{T2}), which targets *Cre* expression to epidermal keratinocytes, have been described (Li et al. 2000). To facilitate cell-type-specific FAK ablation, FAK$^{flox/flox}$ mice were then mated to K14*Cre*ER^{T2} transgenic mice. The resulting offspring carrying K14*Cre*ER^{T2} that were either homozygous for the *floxed* FAK gene (K14*Cre*ER^{T2}/FAK$^{flox/flox}$), carried K14*Cre*ER^{T2} and two copies of the wild-type FAK allele (K14*Cre*ER^{T2}/FAK$^{+/+}$) or the

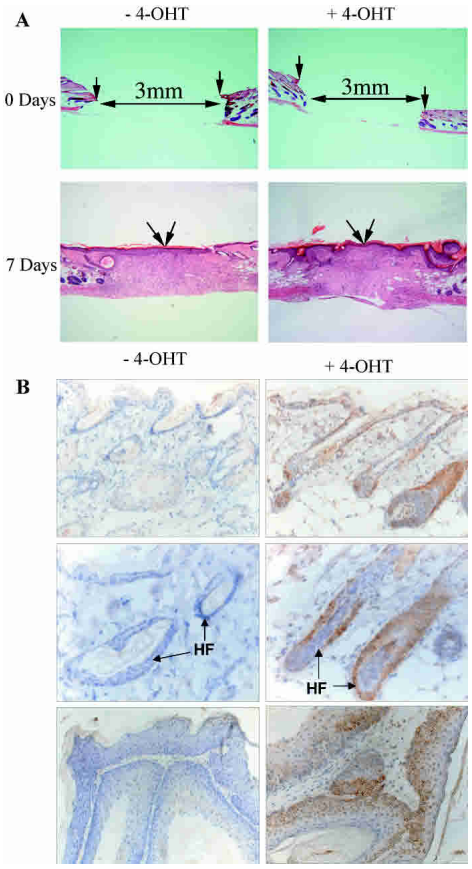

Figure 4. (*A*) Sections of wounded skin from 4-OHT-treated (+4-OHT) or untreated (–4-OHT) K14*Cre*ER^{T2}/FAK$^{flox/flox}$ mice were stained with H&E to examine re-epithelialization at day 0 (*upper* panels) and day 7 (*lower* panels) post-injury. Arrows indicate the leading edges of migrating epidermis. (*B*) Immunohistochemical anti-activated caspase-3 staining of sections of either 4-OHT-treated (+4-OHT) or untreated (–4-OHT) skin (*upper* and *middle* panels) or papillomas (*lower* panels) from K14*Cre*ER^{T2}/FAK$^{flox/flox}$ mice. Images taken at either low (*upper* panels) or high (*middle* and *lower* panels) magnification. (HF) Hair follicles.

FAK *floxed* allele alone ($FAK^{flox/flox}$), were identified by PCR analysis and used for subsequent experiments. All animals used were crossed onto and maintained on an FVB genetic background.

PCR genotyping
Mice that were homozygous for the floxed *fak* gene were routinely identified by PCR analysis. Tail DNA was prepared by standard protocols and subjected to PCR analysis using the following primers: FAK30, 5′-AGAAAGCTATGGAATAGATGAAG-3′ and FAK54, 5′-GTCTGGTGT TCTGAATAAGGTTGG-3′; and the following FAK-specific amplification protocol: 95°C/30 sec (1 cycle); 94°C/10 sec + 57°C/30 sec + 68°C/3 min (10 cycles); 94°C/10 sec + 57°C/30 sec + 68°C/3 min [+20 sec/cycle] (20 cycles); 68°C/7 min (1 cycle). Following amplification, PCR DNA products were digested overnight with HindIII and analyzed by agarose gel electrophoresis. Mice that were homozygous for the floxed *fak* mutation ($FAK^{flox/flox}$) exhibited a single major band of 1.9 kb, mice that were heterozygous for floxed FAK ($FAK^{wt/flox}$) contained two major bands at 1.9 and 1.4 kb, and wild-type (wt) mice ($FAK^{wt/wt}$) contained a single band at 1.4 kb (see Supplemental Material). Mice that additionally contained the K14*Cre*Er^{T2} transgene were again identified by PCR analysis using the following primers: 5′-ATTTGCCTGCATTACCGGTC-3′ and 5′-ATCAACGTTTTCTTTTCGG-3′, and standard amplification protocols. *Cre*-positive mice exhibited a single PCR product of 350 bp.

Preparation and administration of 4-OHT
Preparation and administration of 4-OHT was as described (Indra et al. 1999) except that a reduced dose of 200 µg in 100 µL of sunflower oil was administered. 4-OHT was administered to 8-wk-old female FVB mice as described (Indra et al. 1999), with animals being left for 8–10 d before the initiation of any further experimental procedures. 4-OHT for in vitro experiments was dissolved in ethanol, stored at –20°C, and diluted before use to a final working concentration of 10 nM.

Chemical carcinogenesis
Chemical carcinogenesis using DMBA and TPA was performed on individual study groups of 20 female 8-wk-old animals as previously described (McLean et al. 2001). The number of benign and malignant tumors was recorded weekly for 45 wk after DMBA treatment. Benign tumor numbers did not increase after 24 wk. Upon collection, tumor tissue was either flash frozen in liquid nitrogen or fixed overnight in phosphate-buffered formalin prior to paraffin embedding and histological examination. Tumors were scored as either papillomas or carcinomas by morphological appearance on collection, followed by histological confirmation after H&E staining of paraffin sections. All experiments were carried out in accordance with the United Kingdom Animal Scientific Procedures Act (1986).

Protein analysis
Protein extracts from tissue culture cells or frozen tissue samples were prepared and blotted onto nitrocellulose as previously described (McLean et al. 2001). Membranes were probed with either FAK mAb at 0.5 µg/mL (clone 77; Transduction Laboratories), or anti-tubulin mAb (Calbiochem). Detection was by incubation with horseradish peroxidase-conjugated secondary antibody (New England Biolabs), and visualization was by enhanced chemiluminescence (Amersham Pharmacia Biotech) according to the manufacturer's instructions.

Immunohistochemistry
Rabbit polyclonal antibodies against either FAK (Sigma) or activated caspase-3 (Cell Signalling) were used to stain Formalin Fixed Paraffin Embedded (FFPE) tissue using a two-step immunohistochemical technique. Two-micron-thick FFPE tissue sections mounted onto Superfrost slides (Menzel-Glazer) were dewaxed in HistoClear solution (National Diagnostics) followed by stepped rehydration via a series of graded alcohols to water. A negative control was compared in parallel to the investigated sections by omitting the primary antibody step. Antibody was diluted in 0.1 g of bovine serum albumin (BDH), 0.01 g of Sodium Azide (BDH) in 0.01 M Tris-buffered saline (pH 7.5) and incubated for 2 h at room temperature, followed by visualization with a Cytomation EnVision kit (DAKO) (as per manufacturers' instructions). All staining was performed using a Sequenza (Thermoshandon) semiautomated staining facility. Resulting sections were analyzed and images were captured digitally using a Zeiss Axioskop 50 microscope and Axiovision software version 3.1.

Generation of murine keratinocytes
Primary murine keratinocytes were prepared and propagated from dorsal skin sections of 1- to 2-d-old mice as previously described (McLean et al. 2001). Harvested cells were then plated onto collagen-I precoated tissue culture dishes (Becton Dickinson), and maintained in a humid 37°C/3% CO_2 incubator in keratinocyte growth medium (KGM; Clonetics). For experiments involving *fak* deletion, keratinocytes were pretreated with either 4-OHT (10 nM) in ethanol or vehicle alone, for 48 h with one change of medium and drug at 24 h. This concentration of tamoxifen was identified by titration experiments to be a dose that induced loss of FAK without adverse effects on control cultures.

Wound healing assay
For in vitro wound healing experiments, K14*Cre*Er^{T2}/$FAK^{flox/flox}$ keratinocytes were grown to confluence in 60-mm collagen-I-coated tissue culture dishes (Becton Dickinson) in KGM. Monolayers were wounded using a micropipette tip, and the cells were rinsed with KGM before visualization using a phase-contrast microscope. Cells were treated with either 10 nM 4-OHT or vehicle alone for 48 h before wounding. Wound closure was recorded at 0 and 48 h after 4-OHT removal.

For in vivo wound healing experiments, K14*Cre*ER^{T2}/$FAK^{flox/flox}$ mice were injected intraperitoneally with 4-OHT as described. Mice were allowed to recover for 10 d before wounding. All mice were anesthetized with halothane, and the dorsum was shaved and cleaned with 70% alcohol. Three-millimeter full-thickness cutaneous punch-biopsy wounds were made maintaining the underlying fascia. The wounded tissue was collected at 0 and 7 d post-injury, bisected, and either fixed in 10% formalin at room temperature for 24 h, or in acid alcohol (96% ethanol/1% acetic acid) at 4°C for paraffin embedding, or snap-frozen in OCT (Thermo Lifesciences) and stored at –80°C for cryo-sectioning.

Time-lapse microscopy
K14*Cre*ER^{T2}/$FAK^{flox/flox}$ keratinocytes were harvested as described and plated onto collagen-I-coated six-well tissue culture dishes (Becton Dickinson). Following 4-OHT or vehicle alone treatment, cells were monitored using time-lapse video microscopy with images captured from each well every 20 min over a 10-h period. Quantification of cell motility was achieved by analysis of captured images using cell tracking software (Kenetic Imaging Ltd).

Confocal immunofluorescence microscopy
K14*Cre*ER^{T2}/$FAK^{flox/flox}$ keratinocytes were grown on glass coverslips, fixed at room temperature for 10 min with 3.7% formaldehyde/PBS, and permealized with 0.5% Triton X-100 in PBS and incubated with anti-FAK mAb (Transduction Laboratories). Antibody detection was via fluorescein isothiocynate-conjugated goat anti-mouse IgG (Jackson), for 45 min at room temperature. Fluorescence was visualized using a Bio-Rad MRC 600 confocal microscope.

FACS analysis
K14*Cre*ER^{T2}/$FAK^{flox/flox}$ keratinocytes were either treated with 4-OHT or vehicle alone, washed 1× in PBS, and fixed in 70% ethanol for 3 h at 4°C. Fixed cells were pelleted at 1000 rpm for 5 min, washed 1× in PBS, and resuspended in propidium iodide solution (1 mg/mL). Labeled cell populations were analyzed by fluorescence activated cell sorting (FACS) analysis using a Becton Dickinson Cellquest FACScan.

Acknowledgments

We thank Rebecca Porter for advice and John Wyke and Malcolm Hodgins for critical reading and comments. We also thank Colin Nixon for immunohistochemical analysis. This work was supported by Cancer Research UK at the Beatson Institute (G.W.M., B.S., M.C.F.) and by Collège de France, Association pour la Recherche sur le Cancer, and Foundation pour le Recherche Médicale (D.M. and P.C.).

References

Agochiya, M., Brunton, V.G., Owens, D.W., Parkinson, E.K., Paraskeva, C., Keith, W.N., and Frame, M.C. 1999. Increased dosage and amplification of the focal adhesion kinase gene in human cancer cells. *Oncogene* **18:** 5646–5653.

Argyris, T.S. 1980. Tumour promotion by abrasion induced epidermal hyperplasia in the skin of mice. *J. Invest. Dermatol.* **75:** 360–366.

Burns, F.J., Vanderlaan, M., Snyder, E., and Albert, R.E. 1978. Induction and progression kinetics of mouse skin papillomas. In *Carcinogenesis, mechanisims of tumour promotion and co-carcinogenesis* (eds. T.J. Slaga and R.K. Boutwell), pp. 91–96. Raven Press, New York.

Duan, W.R., Garner, D.S., Williams, S.D., Funckes, C.L., Spath, I.S., and Bloome, E.A. 2003. Comparison of immunohistochemistry for activated caspase-3 and cleaved cytokeratin 18 with the TUNEL method for the quantification of apoptosis in histological sections of PC3 subcutaneous xenographs. *J. Pathol.* **199:** 221–228.

Hauck, C.R., Hsia, D.A., and Schlaepfer, D.D. 2002. The focal adhesion kinase—A regulator of cell migration and invasion. *IUBMB Life* **53:** 115–119.

Ilic, D., Furuta, Y., Kanazawa, S., Takeda, N., Sobue, K., Nakatsuji, N., Nomura, S., Fujimoto, J., Okada, M., and Yamamoto, T. 1995. Reduced cell motility and enhanced focal adhesion contact formation in cells from FAK-deficient mice. *Nature* **377:** 539–544.

Ilic, D., Damsky, C.H., and Yamamoto, T. 1997. Focal adhesion kinase: At the crossroads of signal transduction. *J. Cell Sci.* **110:** 401–407.

Indra, A.K., Warot, X., Brocard, J., Bornert, J.M., Xiao, J.H., Chambon, P., and Metzger, D. 1999. Temporally-controlled site-specific mutagenesis in the basal layer of the epidermis: Comparison of the recombinase activity of the tamoxifen-inducible Cre-ER(T) and Cre-ER(T2) recombinases. *Nucleic Acids Res.* **27:** 4324–4327.

Jones, R.J., Brunton, V.G., and Frame, M.C. 2000. Adhesion-linked kinases in cancer; emphasis on src, focal adhesion kinase and PI 3-kinase. *Eur. J. Cancer* **36:** 1595–1606.

Kemp, C.J., Donehower, L.A., Bradley, A., and Balmain, A. 1993. Reduction of p53 gene dosage does not increase initiation or promotion but enhances malignant progression of chemically induced skin tumors. *Cell* **74:** 813–822.

Li, M., Indra, A.K., Warot, X., Brocard, J., Messaddeq, N., Kato, S., Metzger, D., and Chambon, P. 2000. Skin abnormalities generated by temporally controlled RXRα mutations in mouse epidermis. *Nature* **407:** 633–636.

Marshman, E., Ottewell, P.D., Potten, C.S., and Watson, A.J. 2001. Caspase activation during spontaneous and radiation-induced apoptosis in the murine intestine. *J. Pathol.* **195:** 285–292.

McLean, G.W., Brown, K., Arbuckle, M.I., Wyke, A.W., Pikkarainen, T., Ruoslahti, E., and Frame, M.C. 2001. Decreased focal adhesion kinase suppresses papilloma formation during experimental mouse skin carcinogenesis. *Cancer Res.* **61:** 8385–8389.

McLean, G.W., Avizienyte, E., and Frame, M.C. 2003. Focal adhesion kinase as a potential target in oncology. *Expert Opin. Pharmacother.* **4:** 227–234.

Owens, L.V., Xu, L., Craven, R.J., Dent, G.A., Weiner, T.M., Kornberg, L., Liu, E.T., and Cance, W.G. 1995. Overexpression of the focal adhesion kinase (p125^{FAK}) in invasive human tumors. *Cancer Res.* **55:** 2752–2755.

Owens, L.V., Xu, L., Dent, G.A., Yang, X., Sturge, G.C., Craven, R.J., and Cance, W.G. 1996. Focal adhesion kinase as a marker of invasive potential in differentiated human thyroid cancer. *Ann. Surg. Oncol.* **3:** 100–105.

Pelling, J.C., Fischer, S.M., Neades, R., Strawhecker, J., and Schweickert, L. 1987. Elevated expression and point mutation of the Ha-ras protooncogene in mouse skin tumors promoted by benzoyl peroxide and other promoting agents. *Carcinogenesis* **8:** 1481–1484.

Quintanilla, M., Brown, K., Ramsden, M., and Balmain, A. 1986. Carcinogen-specific mutation and amplification of Ha-ras during mouse skin carcinogenesis. *Nature* **322:** 78–80.

Schaller, M.D. 2001. Biochemical signals and biological responses elicited by the focal adhesion kinase. *Biochim. Biophys. Acta* **1540:** 1–21.

Shibata, K., Kikkawa, F., Nawa, A., Thant, A.A., Naruse, K., Mizutani, S., and Hamaguchi, M. 1998. Both focal adhesion kinase and c-Ras are required for the enhanced matrix metalloproteinase 9 secretion by fibronectin in ovarian cancer cells. *Cancer Res.* **58:** 900–903.

Stoler, A., Kopan, R., Duvic, M., and Fuchs, E. 1988. Use of monospecific antisera and cRNA probes to localize the major changes in keratin expression during normal and abnormal epidermal differentiation. *J. Cell Biol.* **107:** 427–446.

Yuspa, S.H., Hennings, H., Dlugosz, A., Tennenbaum, T., and Glick, A. 1995. The role of growth factors in mouse skin tumor promotion and premalignant progression. *Prog. Clin. Biol. Res.* **391:** 39–48.